ISSN 1674-1056
http://cpb.iphy.ac.cn
http://iopscience.iop.org/cpb
中国物理 B
Chinese Physics
中国物理 Chinese Physics B

Study of effects of imperfect pulses on dynamical decoupling using quantum trajectory method

Lin-Ze He(何林泽), Man-Chao Zhang(张满超), Chun-Wang Wu(吴春旺), Yi Xie(谢艺), Wei Wu(吴伟), Ping-Xing Chen(陈平形)

Citation: Chin. Phys. B . 2018, 27(12): 120303. **doi:** 10.1088/1674-1056/27/12/120303
Journal homepage: http://cpb.iphy.ac.cn; http://iopscience.iop.org/cpb

What follows is a list of articles you may be interested in

Quantum metrology with a non-Markovian qubit system

Jiang Huang(黄江), Wen-Qing Shi(师文庆), Yu-Ping Xie(谢玉萍), Guo-Bao Xu(徐国保), Hui-Xian Wu(巫慧娴)
Chin. Phys. B . 2018, 27(12): 120301. **doi:** 10.1088/1674-1056/27/12/120301

Modulating quantum Fisher information of qubit in dissipative cavity by coupling strength

Danping Lin(林丹萍), Yu Liu(刘禹), Hong-Mei Zou(邹红梅)
Chin. Phys. B . 2018, 27(11): 110303. **doi:** 10.1088/1674-1056/27/11/110303

Non-Gaussianity dynamics of two-mode squeezed number states subject to different types of noise based on cumulant theory

Shaohua Xiang(向少华), Xixiang Zhu(朱喜香), Kehui Song(宋克慧)
Chin. Phys. B . 2018, 27(10): 100305. **doi:** 10.1088/1674-1056/27/10/100305

Quantum speed-up capacity in different types of quantum channels for two-qubit open systems

Wei Wu(吴薇), Xin Liu(刘辛), Chao Wang(王超)
Chin. Phys. B . 2018, 27(6): 060302. **doi:** 10.1088/1674-1056/27/6/060302

Quantum estimation of detection efficiency with no-knowledge quantum feedback

Dong Xie(谢东), Chunling Xu(徐春玲)
Chin. Phys. B . 2018, 27(6): 060303. **doi:** 10.1088/1674-1056/27/6/060303

Effects of imperfect pulses on dynamical decoupling using quantum trajectory method*

Lin-Ze He(何林泽)[1,2,3], Man-Chao Zhang(张满超)[1,2,3], Chun-Wang Wu(吴春旺)[1,2,3], Yi Xie(谢艺)[1,2,3], Wei Wu(吴伟)[1,2,3], and Ping-Xing Chen(陈平形)[1,2,3,†]

[1] *Department of Physics, College of Science and Liberal Arts, National University of Defense Technology, Changsha* 410073, *China*
[2] *Interdisciplinary Center for Quantum Information, National University of Defense Technology, Changsha* 410073, *China*
[3] *State Key Laboratory of High Performance Computing, National University of Defense Technology, Changsha* 410073, *China*

(Received 23 July 2018; revised manuscript received 18 October 2018; published online 10 November 2018)

The dynamical decoupling (DD) method is widely adopted to preserve coherence in different quantum systems. In the case of ideal pulses, its effects on the suppression of noise can be analytically described by the mathematical form of filter function. However, in practical experiments, the unavoidable pulse errors limit the efficiency of DD. In this paper, we study the effects of imperfect pulses on DD efficiency based on quantum trajectories. By directly generating a pseudo noise sequence correlated in time, we can explore the performance of DD with different pulse errors in the typical noise environment. It shows that, for the typical $1/f$ noise environment, the phase error of operational pulses severely affects the performance of noise suppression, while the detuning and intensity errors have less influence. Also, we get the thresholds of these errors for efficient DD under the given experimental conditions. Our method can be widely applied to guide practical DD experimental implementation.

Keywords: pulse imperfections, dynamical decoupling

PACS: 03.65.Yz, 03.67.Pp, 02.60.–x **DOI:** 10.1088/1674-1056/27/12/120303

1. Introduction

Dynamical decoupling (DD), inspired by the application of Hahn echo in nuclear magnetic resonance,[1] is one approach widely used to maintain quantum coherence in various kinds of systems. By exerting a pulse sequence in the quantum evolution process, this method introduces a rapid, time-dependent control field to reduce the interaction with the environment. It was formally introduced in a general way by Viola,[2,3] explaining how a pulse sequence is arranged to compensate the noise effect. After that, several concrete protocols were proposed for different purposes, including periodic DD,[2,3] Carr–Purcell–Meiboom–Gill (CPMG),[4,5] Uhrig DD,[6] and so on. In recent years, different DD protocols have been experimentally demonstrated to preserve the coherence of qubits in trapped ions,[7,8] including the superconducting quantum circuit,[9] electron spins,[10,11] atomic ensembles,[12] semiconductor quantum dots,[13,14] and nitrogen vacancy centers in diamond.[15]

Ideal DD involves a sequence of instantaneous perfect π pulses as the control field, which are used to modulate interaction with the environment. With a tailed pulse sequence, this method can suppress certain frequency components of noise, and its effects can be theoretically described by filter functions. Based on this noise filtering mechanism, qubits can also be used as quantum sensors to detect environment noise.[16] However, unavoidable errors in operational pulses always exist in practical experiments. Even small imperfections, including deviations of pulse width, rotation angle and axis, can have a severe impact on the decoupling efficiency after the accumulation of numerous pulses, which has been pointed out in several works.[8,17–22] Since the pulse errors destroy the symmetry of the DD modulation, we cannot describe this process using concise analytical form like the filter function. Therefore, we use a numerical method to quantitatively analyze the DD process with imperfect pulses.

In this paper, we numerically generate the noise sequence with time correlation according to its power spectral density (PSD).[23] Based on the noise generation, we utilize the quantum trajectory method to numerically study the impacts of imperfections. Different types of pulse error can be directly simulated in the given noise environment to study their effects on DD. The simulated results illustrate that in a typical noise environment, such as $1/f$ noise, phase errors have more influence than detuning and intensity errors and error thresholds decrease with the rise of the pulse number. With these results, we now know how pulse errors influence the DD process in certain environments and this method therefore allows us to instruct various kinds of practical experiments.

The structure of this article is arranged as follows. In Sec-

*Project supported by the National Basic Research Program of China (Grant No. 2016YFA0301903), the National Natural Science Foundation of China (Grant Nos. 11174370, 11304387, 61632021, 11305262, and 61205108), and the Research Plan Project of the National University of Defense Technology (Grant No. ZK16-03-04).

†Corresponding author. E-mail: pxchen@nudt.edu.cn

© 2018 Chinese Physical Society and IOP Publishing Ltd

tion 2, we give a brief review of the theory model about ideal DD in the Ramsey process based on CPMG sequence. In Section 3, a numerical model of imperfect DD is developed, including noise generation, pulse error modeling and quantum trajectory simulation. In Section 4, we compare the noise suppression efficiency of ideal DD and imperfect DD. Finally, a short summary is presented.

2. Theoretical model of ideal DD

In this section, we give the analytical model for ideal DD by simply reviewing the results of Ref. [8]. In the DD operation, there are various kinds of protocols for sequence arrangement. Without loss of generality, the model here is based on the widely used CPMG sequence.[4,5]

The noise suppression effect of DD is usually checked by a modified Ramsey process, with a number of instantaneous π pulses inserted between a pair of Ramsey $\pi/2$ pulses.[24] Particularly, the sequence arrangement of the CPMG protocol is demonstrated in Fig. 1(a). The qubit suffers decoherence caused by ambient noise. The noise can be simply modeled by the energy level drift $\frac{1}{2}f(t)\hat{\sigma}_z$, where $f(t)$ is a random function. The qubit is initialized in $|0\rangle$ state and finally its population of $|0\rangle$ state is measured. By exerting N π pulses between two $\pi/2$ pulses in the time interval $[0,t]$, we can study the noise modulation effects. The CPMG sequence incorporates N evenly spaced π pulses in the time interval $[0,t]$ and the central normalized position of the j_{th} pulse is $\delta_j = (j-1/2)/N$. The time durations of the π pulse and $\pi/2$ pulse are τ_π and $\tau_{\pi/2}$ respectively. Due to their short duration, environmental noise impacts are usually neglected in pulse operation time.

After the first $\pi/2$ pulse, the initial state $|0\rangle$ is prepared to the superposition state $(1/\sqrt{2})(|0\rangle+|1\rangle)$. Here we neglect the global phase of the quantum state because it has no effect on our results. The ambient noise in the time interval $[0,\delta_1 t-\tau_\pi/2]$ will induce random relative phase accumulation between $|0\rangle$ and $|1\rangle$, and the quantum state evolves into $(1/\sqrt{2})(|0\rangle+\mathrm{e}^{-\mathrm{i}\int_0^{\delta_1 t-\tau_\pi/2}f(t')\,\mathrm{d}t'}|1\rangle)$. When the subsequent π pulse is operated, the state is flipped into $(1/\sqrt{2})(|1\rangle+\mathrm{e}^{-\mathrm{i}\int_0^{\delta_1 t-\tau_\pi/2}f(t')\,\mathrm{d}t'}|0\rangle)$. Neglecting an unimportant global phase, it can be written as $(1/\sqrt{2})(|0\rangle+|1\rangle\mathrm{e}^{\mathrm{i}\int_0^{\delta_1 t-\tau_\pi/2}f(t')\,\mathrm{d}t'})$. In the time interval $[\delta_1 t+\tau_\pi/2,\delta_2 t-\tau_\pi/2]$, there is another phase accumulation and the state becomes $(1/\sqrt{2})(|0\rangle+\mathrm{e}^{\mathrm{i}\int_0^{\delta_1 t-\tau_\pi/2}f(t')\,\mathrm{d}t'-\mathrm{i}\int_{\delta_1 t+\tau_\pi/2}^{\delta_2 t-\tau_\pi/2}f(t')\,\mathrm{d}t'}|1\rangle)$. It shows that, in the evolution process, each π pulse changes the phase accumulation direction that is represented by $+1$ and -1, thus offsetting the noise influence. This could be described by a time-domain function $s(t)$, which is the jump function and has values $+1$, -1, and 0 to indicate the error accumulation direction. We have assumed that there is no phase accumulation in π pulse time and $s(t)$ remains 0 during τ_π. Detailed information of the time-domain function $s(t)$ in quantum evolution is shown in Fig. 1(b). Therefore, the final quantum state is written as:

$$\frac{1}{\sqrt{2}}(|0\rangle+\mathrm{e}^{\pm\mathrm{i}\int_0^t s(t')f(t')\,\mathrm{d}t'}|1\rangle), \tag{1}$$

where "$\pm$" corresponds to the situation that N is an odd number and even number respectively.

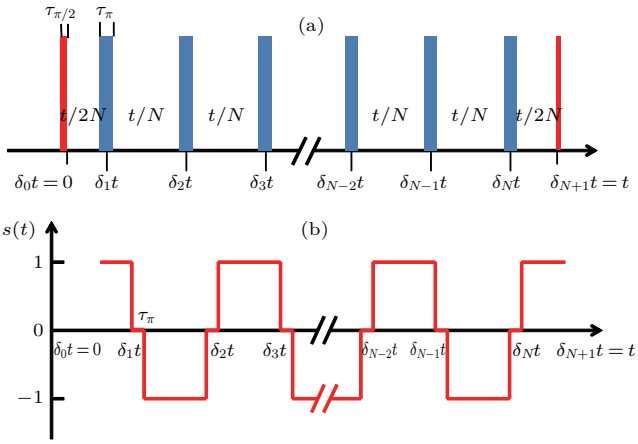


Fig. 1. (color online) (a) CPMG sequence involves N π pulses evenly spaced at the time t between two $\pi/2$ pulses. The time interval between two π pulses is t/N. Each π pulse rotates the quantum state around the x-axis of the Bloch sphere, and the $\pi/2$ pulse rotates the state around the y-axis. (b) During the free-precession period, N π pulses change the phase accumulation direction alternately. It is described by a time-domain jump function $s(t)$, with values indicating the phase accumulation direction. When a π pulse is operated, the value of the function is assumed to be zero.

The state in Eq. (1) is one possible state and is seen as one trajectory. For the final population in $|0\rangle$, we obtain it by applying a $\pi/2$ pulse on the state of Eq. (1) and taking the ensemble average of all trajectories, thus

$$P_0(t)=\frac{1}{2}-\frac{1}{4}\langle\mathrm{e}^{-\mathrm{i}\int_0^t s(t')f(t')\,\mathrm{d}t'}\rangle-\frac{1}{4}\langle\mathrm{e}^{\mathrm{i}\int_0^t s(t')f(t')\,\mathrm{d}t'}\rangle,$$

with $\langle\ \rangle$ representing the ensemble average. In the typical case of Gaussian noise, both the exponential terms $\langle\mathrm{e}^{-\mathrm{i}\int_0^t s(t')f(t')\,\mathrm{d}t'}\rangle$ and $\langle\mathrm{e}^{\mathrm{i}\int_0^t s(t')f(t')\,\mathrm{d}t'}\rangle$ can be transformed into $\exp(-\frac{\int_0^t\int_0^t s(t_1')s(t_2')\langle f(t_1'),f(t_2')\rangle\,\mathrm{d}t_1'\,\mathrm{d}t_2'}{2})$,[20] where $\langle f(t_1'),f(t_2')\rangle$ is the time correlation function of phase noise $f(t)$. Therefore we can obtain

$$P_0(t)=\frac{1}{2}-\frac{1}{2}\exp\left(-\frac{\int_0^t\int_0^t s(t_1')s(t_2')\langle f(t_1'),f(t_2')\rangle\,\mathrm{d}t_1'\,\mathrm{d}t_2'}{2}\right). \tag{2}$$

Introducing the PSD $p(\omega)$ of noise, which is the Fourier transform of $\langle f(t_1'),f(t_2')\rangle$, we can rewrite the integration in the time domain in Eq. (2) into the frequency domain as follows:

$$P_0(t)=\frac{1}{2}-\frac{1}{2}\exp\left(-\frac{t^2}{2\pi}\int_0^\infty G_N(\omega t)p(\omega)\,\mathrm{d}\omega\right), \tag{3}$$

where $G_N(\omega t)$ is the filter function that describes the noise suppression effect of the DD sequence. The mathematical form of the filter function is shown as [25]

$$G_N(\omega t)=\frac{1}{t^2}\mid\mathscr{F}[s(t)]\mid^2$$

$$= \frac{1}{(\omega t)^2} \mid 1+(-1)^{N+1}\exp(-\mathrm{i}\omega t) + 2\sum_{j=1}^{N}(-1)^j \exp(-\mathrm{i}\delta_j \omega t)\cos(\omega\tau_\pi/2) \mid^2, \quad (4)$$

where $\mathscr{F}$ represents the Fourier transform. The value of $G_N(\omega t)$ ranges from 0 to 1 and it plays the role of band pass modulation of noise PSD. If we transform circular frequency to frequency, its band center and band width are determined by $N/2t$ and $1/t$ respectively and they can be modified with a different sequence and time arrangement. In Fig. 2, we plot the filter function $G_N(\omega t)$ with different pulse number N at time intervals of 600 μs.

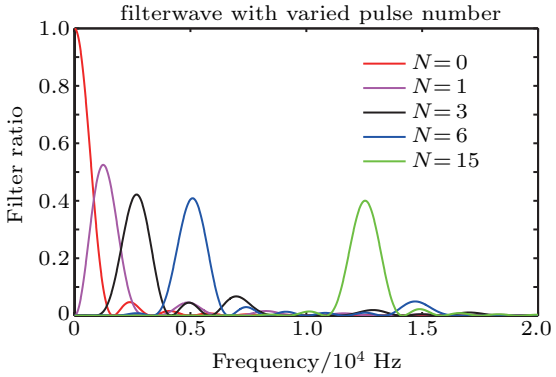


Fig. 2. (color online) Filter functions with various pulse numbers. The filter function has a window of a specific range of frequency while it nearly remains zero in other frequency components, which shows the general effects of noise suppression. When there is no DD pulse, the filter function focuses on the low-frequency range.

The above theoretical model and filter function are derived from ideal pulses, in which case the noise accumulation direction can be described by a concise and symmetrical jump function $s(t)$. However, the imperfections of the pulse will destroy this symmetry, leading to difficulty in obtaining the analytical results. In addition, the imperfections are hard to describe and the accumulation of hundreds of pulses would make the theory form extremely complex. Therefore, a numerical method is required to replace the theoretical model, because it can simulate noise and pulse errors directly, obtaining the evolution results on a large scale of the ensemble average.

3. Numerical model of imperfect DD

In this section, we develop a numerical method for imperfect DD based on the quantum trajectory method. It should be emphasized that, to conveniently consider the time correlation characteristics of the ambient noise, we adopt a semi-classical model to describe the noise.

The quantum trajectory method, also known as the quantum jump method or quantum Monte Carlo wave function method, is one option to simulate quantum dissipation in an open system.[26] The main principle of this method is to evolve the system wave function in time with a pseudo-Hamiltonian, simulating randomization in every time step. The whole process of figuring out one result is called one quantum trajectory and the final result is the ensemble average of many trajectories. To simulate imperfect DD with this method, we must construct the numerical pulse error model and generate the noise sequence.

In the interaction picture and rotating wave approximation, the typical Hamiltonian of a two-level system with pulses in DD can be expressed as

$$H_i = \frac{1}{2}\delta\hat{\boldsymbol{\sigma}}_z + \frac{1}{2}\Omega(\hat{\boldsymbol{\sigma}}^+\exp(-\mathrm{i}\phi) + \hat{\boldsymbol{\sigma}}^-\exp(\mathrm{i}\phi)), \quad (5)$$

where $\hbar = 1$ has been assumed and neglected, δ is the pulse detuning to the resonant frequency of the qubit, Ω is the coupling strength, and ϕ is the phase of the pulse. Because of the instantaneous pulse assumption, we neglect the influence of noise during the pulse time. When there is no pulse, the Hamiltonian is

$$H_\mathrm{d} = \frac{1}{2}(\delta_\mathrm{d} + f(t))\hat{\boldsymbol{\sigma}}_z, \quad (6)$$

where $f(t)$ is a random function and represents the ambient noise which will induce the random phase accumulation and δ_d is the detuning of the $\pi/2$ pulse in the beginning of the evolution.

As is known, any unitary transformation of the qubit state can be described as a rotation of the Bloch vector on the Bloch sphere, $U = \exp(\mathrm{i}k)R_{\boldsymbol{n}}(\theta)$, where $\exp(\mathrm{i}k)$ is a term about the global phase and $R_{\boldsymbol{n}}(\theta)$ is the rotation operator which has a specific form:

$$R_{\boldsymbol{n}}(\theta) = \exp\left(-\mathrm{i}(\boldsymbol{n}\cdot\hat{\boldsymbol{\sigma}})\frac{\theta}{2}\right) = \cos\left(\frac{\theta}{2}\right)\boldsymbol{I} - \mathrm{i}\sin\left(\frac{\theta}{2}\right)(\boldsymbol{n}\cdot\hat{\boldsymbol{\sigma}}), \quad (7)$$

where θ is the rotating angle, $\boldsymbol{n}$ is the rotation axis vector, and $\hat{\boldsymbol{\sigma}}$ is the Pauli operator. In the CPMG sequence, the function of the ideal $\pi/2$ pulse and π pulse correspond to $R_y(\pi/2)$ and $R_x(\pi)$ respectively. On the other hand, the unitary evolution operator according to H_i can be calculated in the form of

$$U_\mathrm{i} = \cos\left(\frac{\sqrt{\delta^2+\Omega^2}t}{2}\right)\hat{\boldsymbol{I}} - \mathrm{i}\sin\left(\frac{\sqrt{\delta^2+\Omega^2}t}{2}\right) \times \left(\frac{\delta}{\sqrt{\delta^2+\Omega^2}}\hat{\boldsymbol{\sigma}}_z + \frac{\Omega}{\sqrt{\delta^2+\Omega^2}}\cos(\phi)\hat{\boldsymbol{\sigma}}_x + \frac{\Omega}{\sqrt{\delta^2+\Omega^2}}\sin(\phi)\hat{\boldsymbol{\sigma}}_y\right). \quad (8)$$

By choosing $\delta = 0$, $\phi = \pi/2$, and $\Omega t = \pi/2$, we have the ideal $\pi/2$ pulse $R_y(\pi/2)$. By choosing $\delta = 0$, $\phi = 0$, and $\Omega t = \pi$, we have the ideal π pulse $R_x(\pi)$.

In this numerical simulation tool, pulse errors are introduced in the form of parameter fluctuations of pulse detuning,

intensity, and phase. Each parameter is fixed in every simulation time step and fluctuates in different time steps. The fluctuations are considered as random terms added to the standard parameter in the simulation. It is shown from Eq. (8) that the parameter fluctuations of detuning and coupling strength contribute to errors in the rotation angle, and parameter fluctuations of detuning, coupling strength, and phase all have impacts on the rotation axis. Because the coupling strength corresponds directly to the laser intensity, the fluctuation of the coupling strength can be seen as a fluctuation of the laser intensity. These parameter fluctuations of pulse are added in the simulation and their influences are then detected according to the decoherence process in Ramsey curves.

In the numerical simulation, every trajectory means the evolution with one possible noise sequence. The corresponding evolution includes the unitary evolution of $H_{\rm d}$ with environmental noise and $H_{\rm i}$ with parameter fluctuations in pulses. The parameter fluctuations are white noise with different standard deviations, while the environmental noise is generated as a noise sequence according to its PSD which is assumed here or obtained from the experiment. To generate it, we discretize the PSD by sampling in its majority range and create frequency spectrum random variables.[22] Then the noise sequence is generated by Fourier transformation into the time domain. Here we choose a typical $1/f$ noise with its PSD $p(f) = 50000/[1+(f/1000)^2]$ to generate a noise sequence and test its effectiveness by PSD estimation.

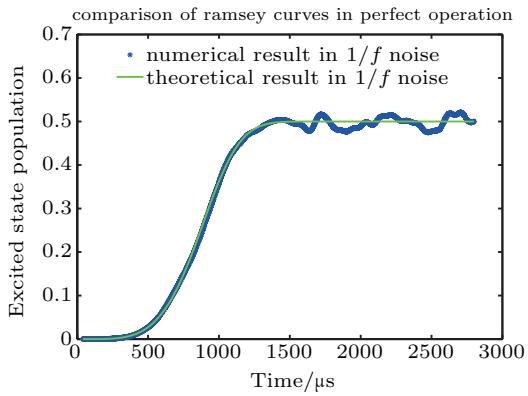


Fig. 3. (color online) Comparison of simulated and theoretical results. For noise with $1/f$ PSD $p(f) = 50000/[1+(f/1000)^2]$, theoretical and numerical results of Ramsey process show nearly perfect fitting and conversely prove the effect of the noise numerical simulation.

In this comparing simulation, we set the ensemble amount as 200. Each trajectory represents a whole Ramsey process with a given noise sequence. Through the trajectory average, this numerical tool simulates the real physical system to the most extent. In the $1/f$ noise environment, the Ramsey process with no pulse is simulated in Fig. 3, showing good compliance with theory, which proves the reliability of our simulation. Situations with pulse errors will be simulated in the next section.

4. Results of the influence of imperfections

To study the impact of pulse errors, we add parameter fluctuations to pulse physical parameters, including detuning, phase, and intensity, which directly influence the coupling strength. The quality of pulses is determined by these pulse parameters and they are set based on general experimental conditions. In the physical parameter arrangement, we assume π pulse detuning δ to be 0 Hz, phase ϕ to be 0, and coupling strength Ω, as well as Rabi frequency, to be 10^6 Hz. In the simulation, number of quantum trajectories is 1000 and we get the ensemble average as the final result. With regard to the noise environment, we choose $1/f$ noise because it is one typical type of noise in the experiment. The $1/f$ noise mainly focuses on the low-frequency components because such noise derives from the fluctuations in electronic devices. Here we adopt a general $1/f$ noise form, with its PSD $p(f) = a/[1+(f/f3)^n]$. Most frequency components and energy is focused within the low-frequency range while only a small proportion of noise power is distributed in the high-frequency range. Therefore, we choose one specific form of PSD $p(f) = 50000/[1+(f/1000)^2]$ to guarantee that most power is concentrated within the low-frequency range. In the simulation, we assume parameter fluctuations to be white noise and Gaussian distributed. Different levels of the standard deviation of parameter fluctuation are set on pulse detuning, phase, and coupling strength. They are written as σ_δ, σ_ϕ, and σ_Ω respectively. With this numerical simulation tool, we explore the general influence of these pulse error sources. But for specific experiments, environmental noise should be detected as a prerequisite and then the particular influence of imperfections can be analyzed to direct the experiment.

We simulate parameter fluctuations of detuning, phase, and coupling strength with 6 and 30 pulses respectively to compare the effects of error accumulation. In consideration of the current experimental developments, we simulate the imperfect DD sequences containing 6 and 30 pulses, which correspond to the cases of short coherence time qubits and relatively long coherence time qubits respectively. With regard to various parameter fluctuation sources, we set different stages based on different σ_δ, σ_ϕ, and σ_Ω on each source to consider how errors influence decoherence. In the simulation, different standard derivations are set in the form of ratio value to Ω. We calculate the Ramsey fringe contrast of every curve and consider the qubit to become decoherent when the fringe contrast is below $1/e$, at about 0.37. For convenience, we simplify the Ramsey fringe contrast as Ψ. According to Eq. (3), we calculate the fringe contrast as $1-2P_0(t)$. Because of the numerical accumulated error, the simulated results of population in the $|0\rangle$ state may slightly deviate from the analytical results and induce a negative contrast value around zero.

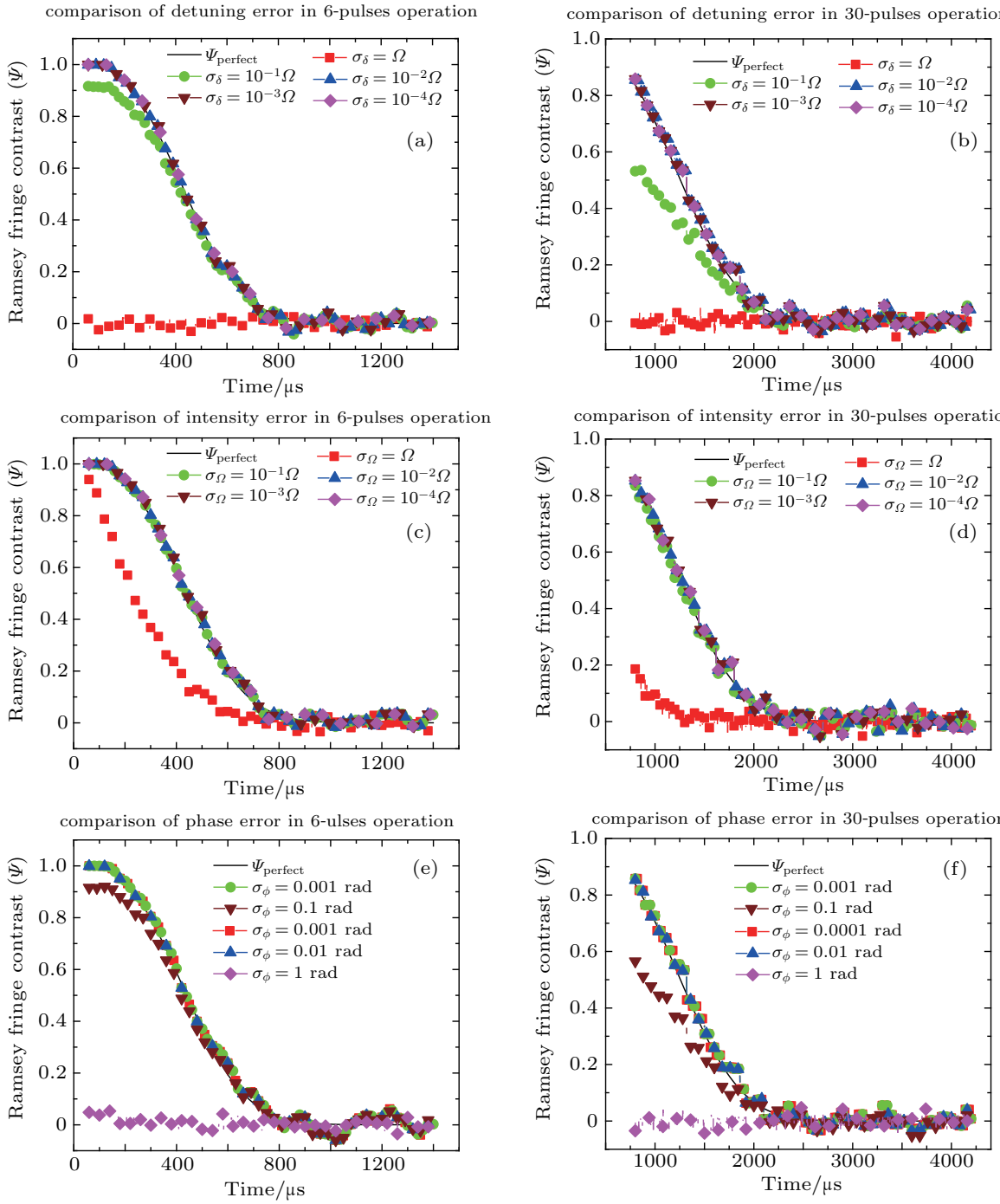


Fig. 4. (color online) (a) and (b) Ramsey fringe contrast with detuning fluctuations in 6 pulses and 30 pulses. We set a series of σ_δ as $10^{-4}\Omega$, $10^{-3}\Omega$, $10^{-2}\Omega$, $10^{-1}\Omega$, and Ω. In the 6-pulse situation, the simulated results of σ_δ that are within $10^{-2}\Omega$ fit well with the perfect results. When σ_δ equals $10^{-1}\Omega$, the simulated result deviates from the perfect result, while for $\sigma_\delta = \Omega$, the qubit becomes decoherent at the beginning. In the 30-pulse situation, the coherent time is prolonged by more pulses. On the other hand, the simulated curves do not fit well with the perfect curve like that in the 6-pulse situation because of the error accumulation. As is shown, for σ_δ within $10^{-2}\Omega$, the results nearly remain the same as the perfect result. For $\sigma_\delta = 10^{-1}\Omega$, the qubit tends to be more liable to dephase than in the situation of 6 pulses. Therefore, the detuning deviation thresholds are approximately $10^{-1}\Omega$ for the 6-pulse operation and tend to be lower than $10^{-1}\Omega$ for the 30-pulse operation. (c) and (d) Ramsey fringe contrast with intensity fluctuations in 6 and 30 pulses. σ_Ω varies among $10^{-4}\Omega$, $10^{-3}\Omega$, $10^{-2}\Omega$, $10^{-1}\Omega$, and Ω. The coherent time of the perfect operation in 6 pulses and 30 pulses is similar to the detuning situation. For the 6-pulse and 30-pulse situations, when σ_Ω does not exceed $10^{-1}\Omega$, the simulated results fit well with the perfect results, but the derivations of the 30-pulse situation are amplified because of the error accumulation. In the 6-pulse situation, the curve of $\sigma_\Omega = \Omega$ is deviates notably from the perfect results, while this trend is exaggerated in the 30-pulse situation. The threshold of fluctuation in pulse intensity is a little below Ω according to these two figures. (e) and (f) Impacts of phase fluctuations with 6 and 30 pulses compared with the perfect operation. We set a series of σ_ϕ as 1 rad, 0.1 rad, 0.01 rad, 0.001 rad, and 0.0001 rad. For Ramsey fringe contrast (Ψ) with 6 pulses in different deviation groups, when σ_ϕ is less than or equal to 0.01 rad, the phase error seems to be less influential on the decoherence and fits well with the perfect results. When σ_ϕ is 0.1 rad, the simulated curve is slightly deviated from the perfect pulse curve. For $\sigma_\phi = 1$ rad, the qubit becomes completely decoherent in the beginning. In the situation of 30 pulses, the influence of errors is notably amplified compared to that with 6 pulses. The qubit is more sensitive to phase noise. When σ_ϕ exceeds 0.1 rad, the coherence is destroyed completely. In addition, for a σ_ϕ of 0.1 rad, the curve is split from the perfect situation clearly. The thresholds of both situations are a little below 0.1 rad.

First we introduce detuning fluctuations and compare their impacts with different pulse accumulation in Fig. 4(a) and Fig. 4(b). As is seen from the figures, the impacts of fluctuations are accumulated with the pulse increasing. For a certain number of pulses and given pulse parameters, there is a threshold for fluctuations, which is assumed to be a little lower than 0.1Ω. When σ_δ does not exceed this threshold, the qubit remains coherent. Therefore, this numerical tool can be used to explore this threshold with different pulse numbers and the given noise environment. In this simulation, the max σ_δ is 10 kHz, which is completely controllable in the experiment. We can be sure that this deviation is within the threshold. As for the fluctuations in coupling strength, with 6 pulses and 30 pulses respectively, the results are shown in Fig. 4(c) and Fig. 4(d). The impacts of σ_Ω are similar to that of detuning, with the error influence amplified by the pulse accumulation. If we consider the DD process in the Bloch sphere, the vector rotation driven by the π pulse represents the offset of noise effects. The phase of the π pulse defines the rotation axis and directly influences the symmetry of the offset. Therefore the phase fluctuations are considered as a vital factor in decoherence. As is seen, decoherence is extremely sensitive to phase error, and even minor noise can easily destroy coherence. We set different levels of fluctuations to check the impact on the final results. Detailed information on the comparison of 6 pulses and 30 pulses is shown in Fig. 4(e) and Fig. 4(f). It shows that the threshold of phase fluctuations is below 0.1 rad.

As phase errors almost determine the length of coherent time, much caution should be applied on this parameter. The preciseness of the pulse phase should be stressed particularly in pulse control. Its electronic error that causes phase instability should also be eliminated completely. Fluctuations in detuning and coupling strength have similar impacts on the evolution process. This is partially because their fluctuation range is tiny compared to the energy level and coupling strength. But it also depends on the real experimental conditions. As a result, we can conclude that the phase noise is the most important error source in the Ramsey process.

The threshold of different kinds of imperfections with different pulse numbers is one important parameter in the experimental implementation. We can compare the fringe contrast between the case of perfect pulses and imperfect pulses with various amounts of fluctuations to get the threshold. As we have defined before, the time when the analytical fringe contrast is around 0.37 is the coherence time. At this time, we observe the fringe contrast of other simulated results and calculate the difference from 0.37. This difference indicates the decoherence caused by pulse imperfections. We can also state that the imperfections have no obvious effects on decoherence if the difference is less than 0.05. The detailed comparison of detuning, intensity or coupling strength, and phase imperfections is shown in Fig. 5. Generally, the difference of fringe contrast would be notably increased if the imperfections were beyond the thresholds. In consideration of the pulse accumulation, the threshold tends to decrease as the pulse number increases.

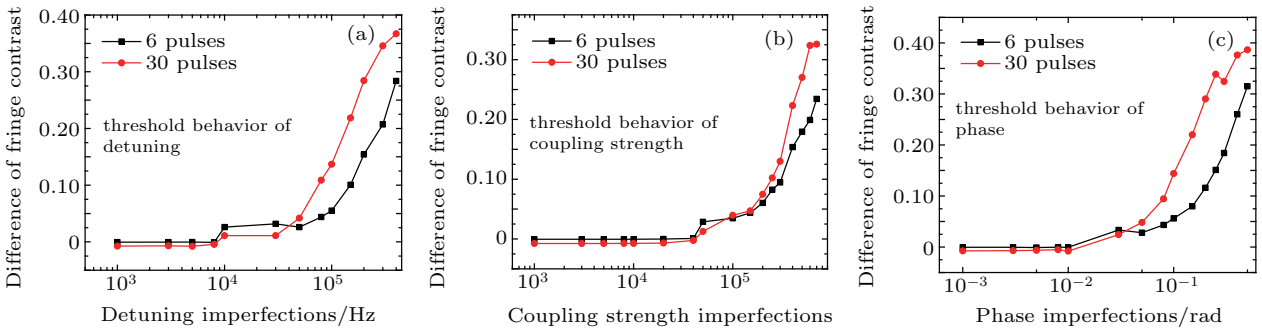


Fig. 5. (color online) (a) Threshold behavior of detuning with imperfections increasing in 6- and 30-pulse situations. Several data points are adopted to show the difference of fringe contrast from the analytical result. For certain detuning imperfections, the fringe contrast difference is increased for the 30-pulse situation because of error accumulation. For the threshold of detuning, the point where the curve rises sharply is around the threshold. As is seen, the detuning threshold for the 6-pulse situation is 5×10^4 Hz and for the 30-pulse situation it is around 3×10^4 Hz. The accumulation of pulses can continuously decrease the thresholds. (b) Threshold behavior of coupling strength, as well as intensity, with imperfections increasing in the 6- and 30-pulse situations. We select many data points that range from 10^3 Hz to 7×10^5 Hz. It is shown that the threshold for the 6-pulse situation is around 1.5×10^5 Hz and for 30 pulses, it is about 3×10^4 Hz. (c) Threshold behavior of phase with imperfections increasing in the 6- and 30-pulse situations. It is shown that the threshold of the phase is 0.05 rad for the 6-pulse situation and 0.01 rad for the 30-pulse situation.

The simulation of pulse imperfections is beneficial to instruct the experimental practice. Our simulation can reveal the thresholds of pulse errors in detuning, intensity, and phase under certain experimental conditions. In practical experiments, the frequency drift, fluctuation in the power of lasers, and phase fluctuation induced by various sources can be monitored as parameter fluctuations. When these fluctuations exceed their thresholds, they are inclined to induce decoherence. The results of the simulation indicate which part of the laser parameters need to be improved and to what extent they need to be optimized. For this reason, we are able to guarantee the efficiency of the DD operation.

5. Summary

We have demonstrated the application of CPMG, for one specific sequence, in the Ramsey process. This process can be

completely described by the theory of filter function, which is determined by the pulse number, time interval between pulses, and pulse operation time. In this process, the quality of pulses is fundamental for the final result as an accumulation of pulse errors would destroy the coherence. Due to the fact that it is difficult to calculate the influence of pulse imperfections, we adopt a numerical method to generate noise to build a numerical tool for the simulation of the Ramsey process. According to the PSD of the noise environment, it is reliable to simulate the whole Ramsey process with the DD sequence. We assume a typical $1/f$ noise environment and simulate the Ramsey process with fluctuations of the pulse parameters. Generally, the quantum state is robust to intensity and detuning errors but extremely sensitive to phase noise. In addition, through simulation, we know the thresholds of the fluctuations of these physical parameters of the pulse. Some improvements can be made to the pulses to reduce fluctuations below the threshold value. Therefore, this simulation tool guides us in improving the experiment, especially when environmental noise is roughly detected by a spectral analyzer. If the pulse noise is designed in the simulation, the results could be an important reference to the real experiment.

Acknowledgments

We would like to thank Professor Pengfei Luo for the discussion on noise simulation. This was the base of the whole simulation. We also thank Professor Uhrig for his guidance in theoretical derivation. Dr. Yanli Zhou also provided us with some suggestions on theoretical derivation.

References

[1] Hahn E L 1950 *Phys. Rev.* **77** 297
[2] Viola L and Lloyd S 1998 *Phys. Rev. A* **58** 2733
[3] Viola L, Knill E and Lloyd S 1999 *Phys. Rev. Lett.* **82** 2417
[4] Carr H Y and Purcell E M 1954 *Phys. Rev.* **94** 630
[5] Meiboom S and Gill D 1958 *Rev. Sci. Instrum.* **29** 688
[6] Gouml and Uhrig G S 2007 *Phys. Rev. Lett.* **98** 100504
[7] Wang Y, Um M, Zhang J H, An S M, Ming L, Zhang J N, Duan L M, Yum D and Kim K 2017 *Nat. Photon.* **11** 646
[8] Biercuk M J, Uys H, Vandevender A P, Shiga N, Itano W M and Bollinger J J 2009 *Nature* **458** 7241
[9] Wang D M, Qian Y, Xu J B and Yu Y H 2015 *Chin. Phys. B* **24** 110304
[10] Du J F, Rong X, Zhao N, Wang Y, Yang J H and Liu R B 2009 *China Basic Science* **461** 7268
[11] Saeedi K, Simmons S, Salvail J Z, Dluhy P, Riemann H, Abrosimov N V, Becker P, Pohl H J, Morton J J and Thewalt M L 2013 *Science* **342** 6160
[12] Sagi Y, Almog I and Davidson N 2010 *Phys. Rev. Lett.* **105** 053201
[13] Bluhm H, Foletti S, Mahalu D, Umansky V and Yacoby A 2009 *Nat. Phys.* **5** 903
[14] Barthel C, Medford J, Marcus C M, Hanson M P and Gossard A C 2010 *Phys. Rev. Lett.* **105** 266808
[15] De L G, Wang Z H, Ristè D, Dobrovitski V V and Hanson R 2010 *Science* **603** 330
[16] Bylander J, Gustavsson S, Yan F, Yoshihara F, Harrabi K, Fitch G, Cory D G, Nakamura Y, Tsai J S and Oliver W D 2011 *Nat. Phys.* **7** 565
[17] Khodjasteh K and Lidar D A 2006 *Phys. Rev. A* **75** 1004
[18] Alvarez G A, Ajoy A, Peng X H and Suter D 2010 *Phys. Rev. A* **82** 042306
[19] Wang Z H, Zhang W X, Tyryshkin A M, Lyon S A, Ager J W, Haller E E and Dobrovitski V V 2012 *Phys. Rev. B* **85** 283
[20] Uhrig G S and Pasini S 2010 *New J. Phys.* **12** 311
[21] Tyryshkin A M, Wang Z H, Zhang W X, Haller E E, Ager J W, Dobrovitski V V and Lyon S A 2010 *J. Phys. B Atomic* **44** 154004 (arXiv: 1011.1903v2 [quant-ph])
[22] Kabytayev C 2015 *Quantum control for time-dependent noise* (Atlanta: Georgia Institute of Technology)
[23] Miller S L and Childers D G 2012 *Probability and Random Processes: With Applications to Signal Processing and Communications* (Academic Press) pp. 164–165
[24] Roos C 2000 *Controlling the quantum state of trapped ions* (Innsbruck: University of Innsbruck)
[25] Lutchyn R M, Cywiński L, Nave C P and Sarma S D 2008 *Phys. Rev. B* **78** 1436
[26] Plenio M B and Knight P L 1998 *Rev. Mod. Phys.* **70** 101